



Contents lists available at ScienceDirect

# Current Research in Pharmacology and Drug Discovery

journal homepage: [www.journals.elsevier.com/current-research-in-pharmacology-and-drug-discovery](http://www.journals.elsevier.com/current-research-in-pharmacology-and-drug-discovery)



## Kinetic conversion of BIOGF1K enriched in compound K from *in vitro* 3-D human tissue model

Woo-Hyun Kim<sup>a,1</sup>, Won-Jo Choi<sup>b,1</sup>, Jeong-Eun Kim<sup>a</sup>, Joonho Choi<sup>c</sup>, Yong-Deok Hong<sup>c</sup>, Jin Nam<sup>c</sup>, Won-Seok Park<sup>c,\*\*</sup>, Soon-Mi Shim<sup>a,\*</sup>

<sup>a</sup> Department of Food Science and Biotechnology, Sejong University, 98 Gunja-dong, Seoul, 05006, South Korea

<sup>b</sup> Department of Agricultural Biotechnology and Research Institute of Agriculture and Life Sciences, Seoul National University, Seoul, 08826, South Korea

<sup>c</sup> AMOREPACIFIC Research and Innovation Center, 1920, Yonggu-daero, Giheung-gu, Yongin-si, 17074, Gyeonggi-do, South Korea

### ARTICLE INFO

#### Keywords:

BIOGF1K  
CK  
CY  
3-D human tissue model  
Skin deposition  
Bioconversion

### ABSTRACT

The purposes of current study were to investigate the effect of ginsenosides from BIOGF1K enriched in compound K (CK) and compound Y (CY) on the skin barrier function, the deposition in *in vitro* 3-D human tissue model (EpiDermFT™ Full Thickness 400), and to identify and quantify kinetic bioconversion of the ginsenosides in artificial skin by utilizing the Fourier transform infrared spectroscopy (FT-IR) and liquid chromatography mass spectrometry (LC-MS), respectively. Epidermal barrier integrity evaluated using transepithelial electrical resistance (TEER) was significantly higher in the BIOGF1K treatment than the CY or CK individual treatment throughout incubation ( $p < 0.05$ ). Skin deposition (%) of CY and CK from BIOGF1K treatment was approximately 4 and 2 times higher than the CY and CK single component treatment, respectively. Total amount of CK found in human skin by deposition and bioconversion was approximately 1087.3, 528.82, and 867.76  $\mu\text{M}$  after topical treatment of BIOGF1K, CK, and CY. Results from the current study reveal that topical treatment of BIOGF1K more effectively induced CK deposition as well as bioconversion of CY to CK than that of a single treatment of CY or CK, suggesting that BIOGF1K could be a useful cosmetic preparation for enhancing skin function.

### 1. Introduction

Ginsenosides are major phytochemical derived from ginseng (*Panax ginseng*), and they are traditionally used as pharmaceutical agents (Moon, 2018). They are divided into protopanaxadiol (PPD), which include Rd, Rb, Rh2, and Rg3 and protopanaxatriol (PPT) types, such as Rg1, Rh1, and Re, which are based on the structure of the ginsenosides (Nam et al., 2013; Zhou, 2008). Recent studies proved their metabolites on skin health, including anti-aging, wound healing, and protection from ultraviolet irradiation (Lim, 2015). They also demonstrated the beneficial effects of ginsenosides. It was reported that ginsenoside compound K (CK) among ginsenosides provided various cosmetic effects on skin health, including treatment of such barrier-disrupted diseases as atopic dermatitis. This suggests that it might be a candidate for cosmetic applications (Hong, 2018; Lee, 2003).

BIOGF1K, which is a hydrolyzed ginsenoside fraction from the root of *Panax ginseng*, is rich in CK, and it also contains compound Y (CY),

MC, F1, F2, Rd, and Rg1 (Kim, 2023). It is widely used for cosmetic purposes in Korea owing to its diverse biological effects on skin (Hossen, 2017). For instance, several studies discovered that BIOGF1K played an important role in inhibiting inflammation, photoaging, and atopic dermatitis in skin (Hong, 2018; Kim, 2018). CK attached to the smallest number of glycoside among PPD was particularly the most abundant in BIOGF1K, and it was found to increase hyaluronan synthase, resulting in anti-aging by helping preserve skin homeostasis via aging (Lim, 2015). It was observed that CK from BIOGF1K quickly entered into the epidermal barrier, which contributed to the skin barrier function in an HaCaT cell (Kim, 2023). The study also proposed that CY was the second highest substance in BIOGF1K, and it could be converted to CK when BIOGF1K permeated into the epidermis in an HaCaT cell.

It is necessary to elucidate deposition and bioconversion of ginsenosides in epidermis-dermis in order to increase its spectrum of biological activities. The skin deposition or bioconversion of ginsenosides from BIOGF1K, particularly CY to CK in epidermis-dermis skin has not

\* Corresponding author.

\*\* Corresponding author.

E-mail addresses: [wspark@amorepacific.com](mailto:wspark@amorepacific.com) (W.-S. Park), [soonmishim@sejong.ac.kr](mailto:soonmishim@sejong.ac.kr) (S.-M. Shim).

<sup>1</sup> Co-first authors: Won-Jo Choi and Woo-Hyun Kim equally contributed to the current study.

<https://doi.org/10.1016/j.crphar.2023.100165>

Received 4 September 2023; Received in revised form 9 October 2023; Accepted 10 October 2023

Available online 12 October 2023

2590-2571/© 2023 Published by Elsevier B.V. This is an open access article under the CC BY-NC-ND license (<http://creativecommons.org/licenses/by-nc-nd/4.0/>).

been reported yet to the best of our knowledge. Hence, the objective of the current study was to investigate the effect of BIOGF1K and its major components, including CK and CY, on the epidermal barrier integrity, skin deposition, and bioconversion in *in vitro* 3-D human tissue models (EpiDermFT™ Full Thickness 400). The current study identified the spectral differentiation of the ginsenoside metabolites produced in artificial epidermis-dermis skin by utilizing the Fourier transform infrared spectroscopy (FT-IR) as well as quantified deposition of metabolites after topical treatment of BIOGF1K, CY, and CK using liquid chromatography mass spectrometry (LC-MS).

## 2. Materials and methods

### 2.1. Chemicals and reagents

Ginsenoside CK and CY standards were purchased from Ambo Institute (Daejeon, Korea). The acetonitrile (ACN), methanol, and water with a grade for HPLC were obtained from J.T. Baker (Phillipsburg, NJ, USA). All chemicals were analytical grades, and they were stored in compliance with the shelf life and storage conditions.

### 2.2. Preparation of hydrolyzed ginsenoside-rich fraction, BIOGF1K

BIOGF1K, a hydrolyzed ginsenoside-rich fraction, was gifted by AMOREPACIFIC (Yongsan-gu, Seoul). BIOGF1K was dissolved in ethanol at 100 mg/mL as a stock solution and diluted to DMEM for treatment of BIOGF1K to cell culture.

### 2.3. Transport study of BIOGF1K using a human artificial skin equivalent model

An *in vitro* 3-D human tissue model, EpiDermFT™ Full Thickness 400 (EFT-400) artificial skin model was purchased from MatTek Corporation (Ashland, MA, USA), which consisted of human-derived epidermal keratinocytes and human-derived dermal fibroblasts that were grown on a semi-permeable membrane. The EFT-400 skin tissue inserts were transferred to 6-well plates containing 2.5 mL of serum-free medium (EFT-400-ASY) upon arrival. The tissues were then equilibrated at 37 °C under 5% a CO<sub>2</sub> atmosphere condition overnight. The medium was aspirated and replaced with a fresh pre-warmed media after the equilibrations. The EFT-400 skin tissues were incubated with 5000 µg/mL of BIOGF1K, 2500 µg/mL of compound Y and compound K or control culture media for a maximum of 2 h for the experiments. The tissues were then harvested using an NP40 cell lysis buffer (Invitrogen, Thermo Fisher Scientific) for further analyses after treatment.

The values of the trans-epithelial electrical resistance (TEER) were measured using a Millicell® ERS-2 Volt ohmmeter (Merck Millipore Corp., Burlington, MA, USA) in order to investigate the effect of BIOGF1K on the skin barrier integrity of artificial skins. The TEER values were measured at the following time points: 0, 2, 4, 8, and 24 h. The treated EFT-400 skin tissues were washed with Dulbecco's phosphate buffered saline (DPBS; Corning Inc; MA; USA) and homogenized using an NP40 cell lysis buffer (Invitrogen; Thermo Fisher Scientific; MA; USA) and a homogenizer (HG-15 A; Daihan Scientific Co. Ltd, Wonju-si, Gangwon-do, Republic of Korea) for further analyses after treatment for 2 h, which is the mid-time point, and 24 h, the end-time point. The homogenized samples were centrifuged at 4 °C and 4000 rpm for 15 min.

### 2.4. Quantitative analysis of BIOGF1K, CK, and CY using HPLC

The identification of the ginsenosides in BIOGF1K and its metabolites was performed by high performance liquid chromatography (HPLC)-UV (ThermoFisher, Waltham, USA) according to a previous method with modifications (Hossen, 2017; Yeom, 2010). The reverse phase column, Mightysil RP-18 GP (4.6 × 250 mm, 5 µm; Kanto chemical, Tokyo,

Japan) column, was used and the column oven was set to 40 °C. The stock solution of the ginsenoside CK standard was made using 100% methanol, which was diluted in 50% methanol, and it was then filtered using 0.45 µm polytetrafluoroethylene (PTFE) syringe filters. The gradients of the mobile phase were 10% acetonitrile (A) and 90% acetonitrile (B), which included 0–10 min for 15% B, 10–50 min for 15–60% B, 50–70 min for 60–85% B, 70–71 min for 85–15% B, and 71–80 min for 15% B. The sample injection volume was 10 µL.

### 2.5. Analysis of the FT-IR spectra of artificial skins with BIOGF1K

Percentage of transmittance from samples were recorded on an infrared spectrometer (Thermo Fisher Scientific) over a wavelength range of 400–4000/cm via the attenuated total reflection (ATR) method. The investigational data of FT-IR was analyzed using OMNIC software, and the absorption peaks were recorded.

### 2.6. Statistical analysis

Data obtained from triplicate experiments were described as mean ± standard deviation (SD). Tukey's test and a one-way analysis of variance (ANOVA) were statistically applied in order to confirm the significance of the differences ( $p < 0.05$ ) using GraphPad Prism 6.0 software (San Diego, CA, USA).

## 3. Results

### 3.1. Changes in the cellular integrity of 3-D human tissue model after treatment of BIOGF1K, CK, and CY

Changes in the cellular integrity measured using TEER from EFT-400 at 0, 2, 4, 8, and 24 h after the topical application of BIOGF1K, CK, and CY are shown in Fig. 1. The TEER value that was obtained from the treatment of a single component of CY or CK was normalized according to the content of CY and CK from BIOGF1K in order to compare the relative effect on the cellular integrity. Overall, a remarkable reduction in TEER value occurred at 2 h and then recovered during incubation time. The TEER value was  $88.48 \pm 12.16\%$ ,  $18.73 \pm 1.03\%$ , and  $46.25 \pm 14.13\%$  of the initial time after treatment of BIOGF1K, CY, and CK treatment, respectively (Fig. 1). When compared to epidermal integrity between single components, the topical treatment of CK provided a significantly higher TEER value than CY at each incubation time ( $p < 0.05$ ). The topical treatment of BIOGF1K showed significantly higher value of TEER than that of CY and CK for 24 h incubation ( $p < 0.05$ ).

Deposition of BIOGF1K, CY, and CK in EpiDermFT™ Full Thickness 400.

The skin deposition (%) of CK and CY after topical treatment of BIOGF1K or single component of CK and CY in the 3-D human tissue model is illustrated in Fig. 2. CK and CY, as major components in BIOGF1K, appeared to increase via the incubation time. Other ginsenosides contained in BIOGF1K were not detected in the 3-D human tissue model after treatment of BIOGF1K. The artificial skin deposition(%) after the BIOGF1K treatment showed 27% at 2 h and 40% at 24 h for CY as depicted in Figs. 2A and 37% at 2 h and 43% at 24 h for CK in Fig. 2B. The skin deposition (%) of CY and CK from the BIOGF1K treatment was approximately 4 and 2 times higher than that of a single CY (7%) and CK (22%) component treatment after 2 h of incubation (Fig. 2). However, there was no significant difference in skin deposition of CY and CK between BIOGF1K and a single component of CY or CK after 24 h topical treatment ( $p > 0.05$ ). The results indicate that CY and CK from BIOGF1K is more likely to be rapidly and highly permeable than its single topical treatment of CK or CY in 3-D human tissue model. Hence, the current study further identified the spectral differentiation of the metabolites that are produced in *in vitro* 3-D human tissue model skin after topical treatment of BIOGF1K, CK, and CY by utilizing FT-IR.

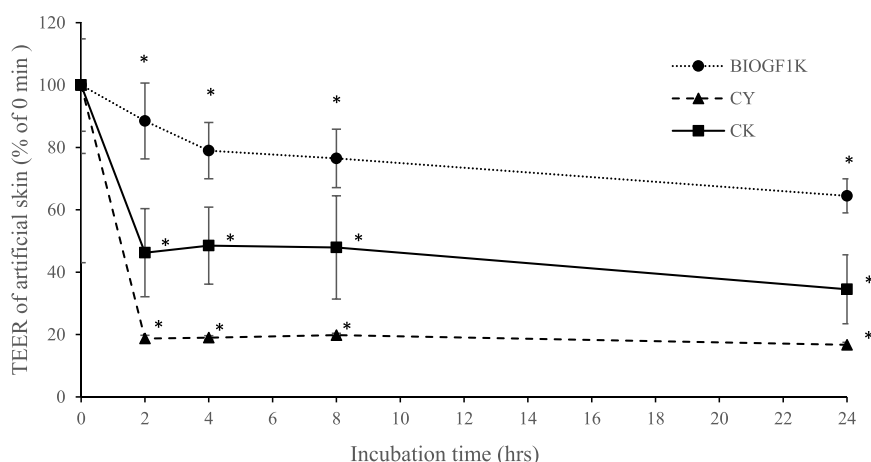


**Fig. 1.** Changes in the cellular integrity of artificial skin after a topical application of 5000  $\mu\text{g}/\text{mL}$  BIOGF1K, 2500  $\mu\text{g}/\text{mL}$  compound Y (CY) and 2500  $\mu\text{g}/\text{mL}$  compound K (CK). The control indicates artificial skin without any treatments. An asterisk (\*) indicates a significant difference compared to the control ( $*p < 0.05$ ). The different letters indicate a significant difference among the ginsenosides treatments at each time point of incubation ( $p < 0.05$ ).

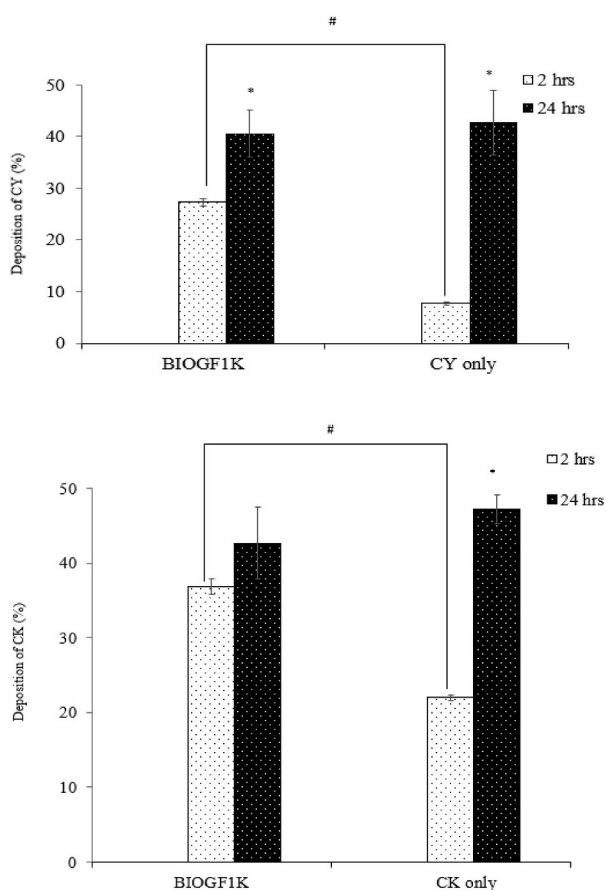


**Fig. 2.** Deposition of CY after incubating 5000  $\mu\text{g}/\text{mL}$  BIOGF1K and 2500  $\mu\text{g}/\text{mL}$  CY (A) and CK after incubating 5000  $\mu\text{g}/\text{mL}$  BIOGF1K and 2500  $\mu\text{g}/\text{mL}$  CK (B) by EFT-400. An asterisk (\*) indicates a significant difference between incubation times ( $*p < 0.05$ ). The # on the bar indicates a significant difference between treatments in the same incubation time ( $p < 0.05$ ).

### 3.2. Spectral identification of the bioconversion from CY to CK

FT-IR analyses were conducted in order to identify the bioconversion from CY to CK after the treatment of CY only by measuring the structural changes, as illustrated in Fig. 3. Firstly, the FT-IR signatures of each

**A**

BIOGF1K, CY, and CK were spectrally identified, showing the absorption peak of O–H stretching at wavenumbers of 3314  $\text{cm}^{-1}$ , 3321  $\text{cm}^{-1}$ , and 3313  $\text{cm}^{-1}$  for BIOGF1K, a single component of CY, and a single component of CK, respectively (Fig. 3A). The result corresponds with a previous finding in which a broad band between 3200 and 3600  $\text{cm}^{-1}$  was ascribed to O–H stretching, which is related to intramolecular and intermolecular hydrogen bonds (Oh et al., 2021). After 24 h topical treatment of BIOGF1K and CY single component in the 3-D human tissue model, the absorption peak of O–H stretching was red-shifted from 3314 to 3321  $\text{cm}^{-1}$  to 3274 and 3308  $\text{cm}^{-1}$  respectively (Fig. 3B). The change in value of wave numbers of BIOGF1K ( $\Delta 40$ ) was greater than that of CY ( $\Delta 13$ ). In contrast to treatment of BIOGF1K and CY single component, the absorption peak of O–H stretching from treatment of CK single component was blue-shifted from 3313 to 3321  $\text{cm}^{-1}$  (Fig. 3B). In the case of receiver compartment after 24 h topical treatment, it was red-shifted in all treatments, but the change value in wave numbers was greater in BIOGF1K than CY or CK single component (Fig. 3C).

**B**

### 3.3. Mass identification and quantification of the bioconversion from CY to CK

The skin from the EpiDermFT™ culture was collected for 2 and 24 h after the topical treatment of CY in order to identify the bioconversion of CY to CK. The total ion chromatography (TIC) from each skin sample was detected at 64.68 min after 2-hr incubation (Fig. 4A) and 64.84 min after 24 h incubation time (Fig. 4B). Mass to charge ratio ( $m/z$ ) was 465.38  $m/z$  and 203.26  $m/z$  at 64.68 and 64.84 min, respectively, indicating that the product ion produced from CK. A similar finding was reported that several fragmentation products with having  $m/z$  465.31, 203.15 were identified by MS/MS fragmentation for CK,  $m/z$  645.91 [M + Na] at 62.81 min of retention time (Yang, 2015). The amount of bio-converted CK after the treatment of CY in the artificial skin were approximately 867.73  $\mu\text{M}$  and 872.33  $\mu\text{M}$ , which is approximately 26.12% and 26.25% of CY for 2 h and 24 h, respectively (Fig. 5). The results indicate that the bioconversion from CY into CK on the epidermis-dermis skin continuously occurred for 24 h incubation time.

## 4. Discussion

Our group previously not only identified the major components from BIOGF1K such as CY and CK but also quantified the  $93.49 \pm 1.60$  of CY and  $343.38 \pm 4.76$  mg/g of CK (Kim, 2023). That study also found comparable results to the current study in that BIOGF1K enriched in CK and CY was effective in regards to improving the epidermis barrier

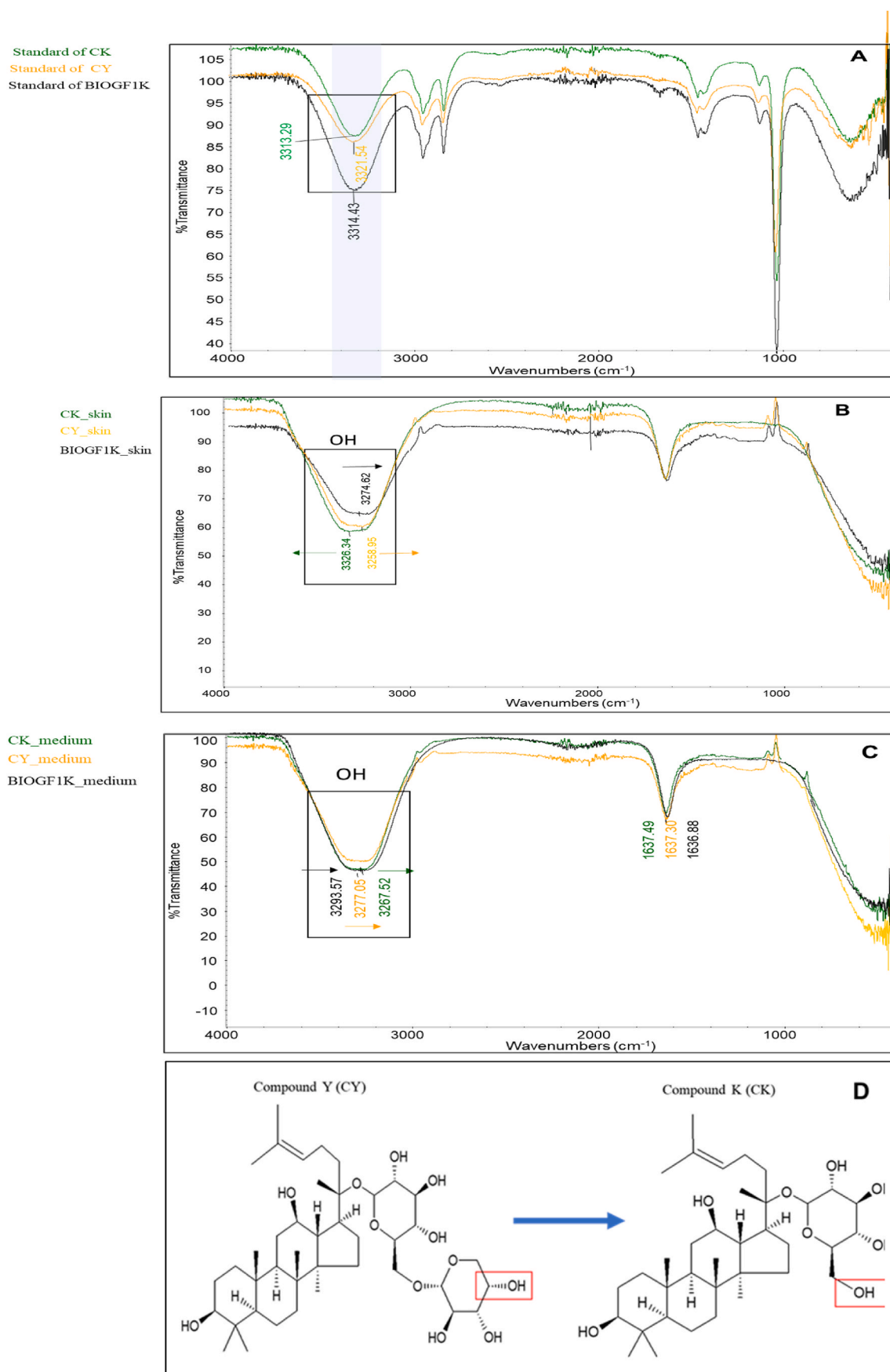


**Fig. 3.** FT-IR spectral signatures and spectral features of BIOGF1K and the standard of compound K (CK), compound Y (CY) standard (A), artificial skin (B), and basal medium (C) after the topical application of 5000 µg/mL BIOGF1K, 2500 µg/mL CK, and 2500 µg/mL CY in the EpiDermFT™ culture.

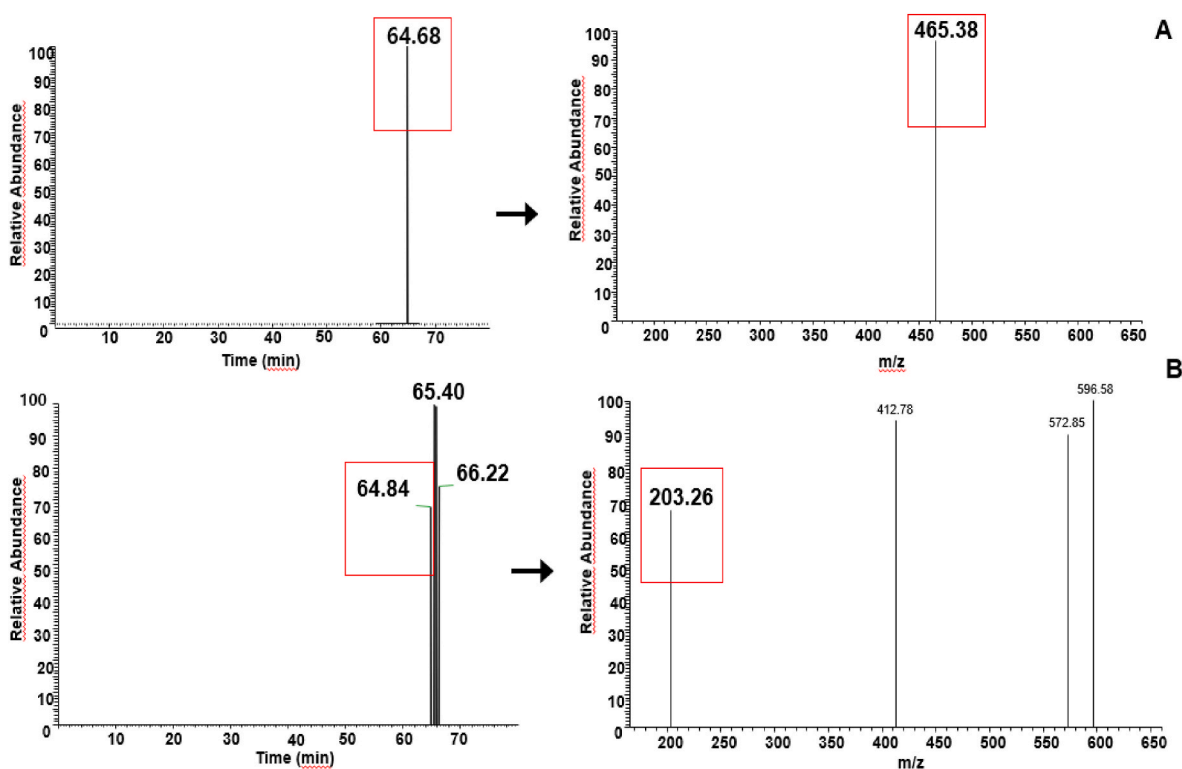


Fig. 4. Total ion chromatography (TIC) from EpiDermFT™ culture after the topical application of 2500  $\mu\text{g}/\text{mL}$  compound Y (CY) at 2hr and its mass spectra (MS<sub>2</sub>) @ 64.68 min (A) and the TIC of compound Y (CY) at 24 h and its MS<sub>2</sub> @ 64.84 min (B).

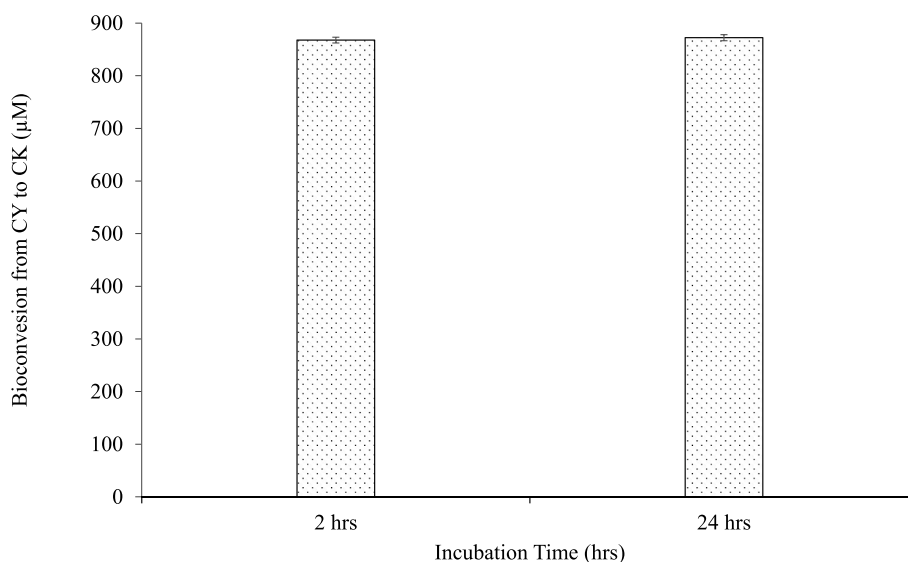


Fig. 5. Bioconversion from compound Y (CY) to compound K (CK) in the EpiDermFT™ culture.

function of keratinocytes using the HaCaT cell line (Kim, 2023). The skin barrier is known to play an important role in regards to protecting water, proteins, and electrolytes from being lost (Park et al., 2020). In addition, it is useful for treating barrier-disrupted diseases, such as atopic dermatitis as well as establishing the integrity of the skin (Brandner, 2016).

Our findings that CY and CK from BIOGF1K is more likely to be permeated faster and higher than its single topical treatment of CK or CY in 3-D human tissue model. The result implies that topical treatment of BIOGF1K, which is not only in enriched CK but also contains CY and other ginsenosides, could be effective on enhancing skin barrier function

of epidermis-dermis than that of a single component of CY or CK. A previous study supported the finding that bioactive components from plant extracts absorb better than with a single substance due to interaction or synergic effects of the matrix and components during metabolism when used as an extract (Shkemi and Huppertz, 2021). To the best of our knowledge, the skin function between a single CY and CK component has not yet been compared, but several studies reported that BIOGF1K provided skin protective activities by inhibiting inflammation and oxidation because it is rich in CK (Lim, 2015; Hossen, 2017). Results from our study suggest that BIOGF1K could provide a more positive skin effect than a single treatment of CY or CK in the epidermis and dermis

due to highly effective skin deposition of CY and CK. This is because the content of CK was higher than CY from BIOGF1K, and it is plausible that CY, which is the second most predominant component in BIOGF1K, could be converted into CK in human tissue. The result from a previous study also confirmed that CY from BIOGF1K could be converted to CK when BIOGF1K permeated into the epidermis by using HaCaT cell (Kim, 2023).

As arabinose pyranose which has several R-OH is eliminated from CY among the main components of BIOGF1K, hydrogen bonds (O-H) are formed by interacting with surrounding molecules, and the length of hydrogen bonds increases as the formation position of hydrogen bonds changes. Similar findings were reported that one sugar arabinose pyranose is eliminated from CY due to hydrolysis and it affects the formation of hydrogen bonds (O-H) according to interact with the surrounding molecules (Ramírez-Hernández et al., 2019; Tian et al., 2023; Li et al., 2002). As the distance between oxygen and hydrogen atoms increases, the force of oxygen atoms to attract charges weakens, reducing the dispersion of charges, which is expected to result in red shift due to lower vibration frequencies caused by hydrogen bonds. In other words, it is possible that CY as one of the major ingredients from BIOGF1K could convert to CK, which is a less polar ginsenoside by a lost specific molecular. It is supported by the transformation of ginsenosides that occur in the PPD group, such as CY, Rb1, and Rb2 increased the amount of CK (Li, 2022). Moreover, those changes in inter and intra molecular interactions was more strongly occurred from BIOGF1K than CY. Hence, the possibility of bioconversion from CY to CK, we further identified and quantified the amount of bioconversion from CY to CK by LC/MS-TIC after topical treatment of CY in 3-D human tissue.

The PPD ginsenosides were generally hydrolyzed by an intestinal microorganism or hydrolases, for example pectinase and  $\beta$ -glycosidase (Yang, 2015). It is known that CY can be hydrolyzed into CK by recombinant  $\beta$ -glycosidase from *Sulfolobus solfataricus* and *Microbacterium esteraromaticum* (Noh and Oh, 2009; Quan, 2012). Various enzymes including aldehyde dehydrogenase (ADH), alcohol dehydrogenase (ALDH), and cytochrome P450 (CYP), as well as millions of bacteria, fungi, and viruses that compose of the skin microbiota were found in artificial skin (Byrd et al., 2018; Pyo and Maibach, 2019). Carboxylesterases surpass the activity of arylesterase, and betamethasone 17-valerate is a substrate of carboxylesterases (Bätz et al., 2013). Protopanaxadiol (PPD) ginsenosides exhibited strong inhibition on carboxylesterases (Sun et al., 2019). These enzymes and microbiome could probably be involved in the biotransformation of applied ginsenosides in

3-D human tissue model.

Our group previously found CK was found to be the one of prominent ingredients from BIOGF1K for protecting skin aging (Lim, 2015). According to findings from the current study on the deposition and bioconversion rates, the total amount of CK found in human skin by deposition and bioconversion from CY after topical treatment of BIOGF1K, CK, and CY in the 3-D human skin model was estimated (Fig. 6). When BIOGF1K was topically treated into human skin, approximately 1087.3  $\mu\text{M}$  of CK was found by considering 37% of the CK deposition rate and 26.12% of the bioconversion rate from CY to CK at 2 h. However, only 528.82  $\mu\text{M}$  was deposited in skin without any bioconversion when CK as a single component was topically treated into skin. In the case of topical treatment of CY, approximately 867.76  $\mu\text{M}$  of CK was found by considering that 40% of CY was accumulated in skin and then its 26.25% was converted to CK. Likewise, 1281.2, 1136.62, and 872.33  $\mu\text{M}$  of CK is found in human skin after 24-hr topical treatment of BIOGF1K, CK, and CY, respectively (Fig. 6). Taken together, BIOGF1K, which mainly contains CK as well as CY, could be superior to a single treatment of either CK or CY for skin health by enhancing skin deposition and bioconversion from CY to CK.

## 5. Conclusions

The epidermal barrier integrity of the 3-D human tissue model was highly maintained and recovered by topical treatment of BIOGF1K, enriched in CK compared to the CK or CY single component. Skin deposition of CY or CK was higher from the topical treatment of BIOGF1K compared to either the CY or CK single treatment. It was characterized that CY, which is second most contained component in BIOGF1K, was bio-converted to CK by detaching a molecule having an O-H bond and spectral changes was higher in BIOGF1K than in CY single treatment. Approximately 26.12% and 26.25% of CY was converted to CK after 2 and 24 h of CY topical treatment. Our findings suggest that BIOGF1K could be a useful cosmetic preparation in regards to enhancing skin function due to effective skin deposition of CK and the bioconversion of CY to CK. Further studies are required to elucidate which enzymes or microbiomes are responsible for promoting the biotransformation of CY to CK after topical treatment of BIOGF1K in epidermal-dermis tissue.

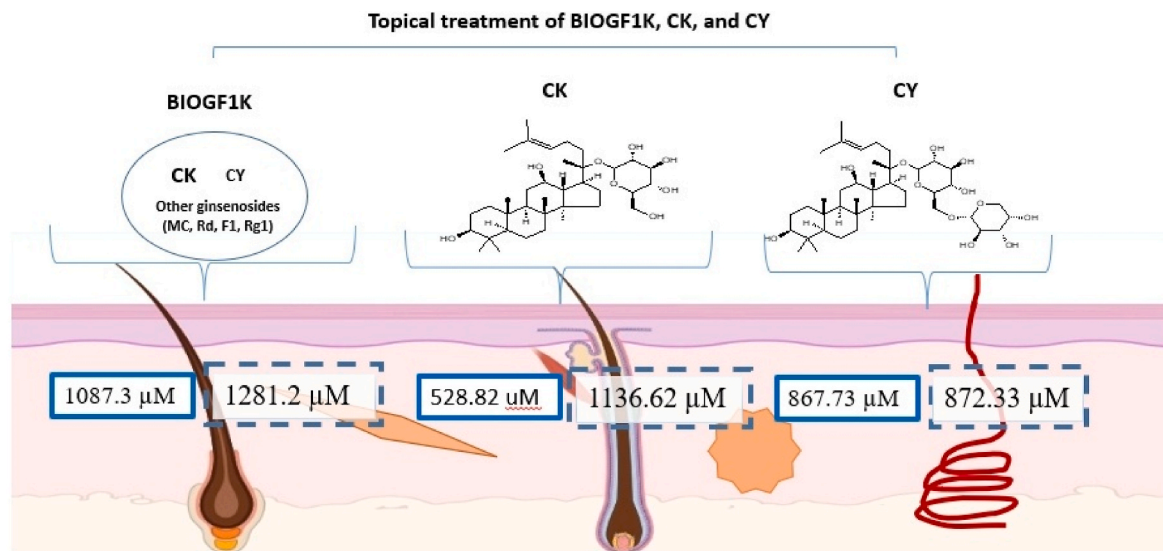


Fig. 6. Total amount of CK found in skin by deposition and bioconversion from CY after topical treatment of 5000  $\mu\text{g}/\text{mL}$  BIOGF1K, 2500  $\mu\text{g}/\text{mL}$  CK, and 2500  $\mu\text{g}/\text{mL}$  CY in 3-D human skin model (solid line box: 2hrs after treatment; dotted line box: 24 h after treatment).

**Declaration of competing interest**

None

**Data availability**

Data will be made available on request.

**Acknowledgement**

The current study was financially supported by the AMOREPACIFIC Research and Innovation Center in 2022.

**References**

- Bätz, F.M., Klipper, W., Korting, H.C., Henkler, F., Landsiedel, R., Luch, A., et al., 2013. Esterase activity in excised and reconstructed human skin—biotransformation of prednicarbate and the model dye fluorescein diacetate. *Eur. J. Pharm. Biopharm.* 84 (2), 374–385.
- Brandner, J.M., 2016. Importance of tight junctions in relation to skin barrier function. *Skin Barrier Function* 49, 27–37.
- Byrd, A.L., Belkaid, Y., Segre, J.A., 2018. The human skin microbiome. *Nature Rev. Microbiol.* 16 (3), 143–155.
- Hong, Y.H., 2018. Photoaging protective effects of BIOGF1K, a compound-K-rich fraction prepared from panax ginseng. *J. Ginseng Res.* 42 (1), 81–89.
- Hossen, 2017. *In vitro* antioxidative and anti-inflammatory effects of the compound K-rich fraction BIOGF1K, prepared from Panax ginseng. *J. Ginseng Res.* 41 (1), 43–51, 2017.
- Kim, E., 2018. BIOGF1K, a compound K-rich fraction of ginseng, plays an antiinflammatory role by targeting an activator protein-1 signaling pathway in RAW264.7 macrophage-like cells. *J. Ginseng Res.* 42 (2), 233.
- Kim, W.H., 2023. Bioconversion of hydrolyzed ginsenoside-rich fraction from ginseng root and its effect on epidermal barrier function. *Heliyon* 9, 4.
- Lee, E.H., 2003. Ginsenoside F1 protects human HaCaT keratinocytes from ultraviolet-B-induced apoptosis by maintaining constant levels of Bcl-2. *J. Invest. Dermatol.* 121 (3), 607–613.
- Li, R., 2022. Co-immobilized  $\beta$ -glucosidase and snailase in green synthesized Zn-BTC for ginsenoside CK biocatalysis. *Biochem. Eng. J.* 188, 108677.
- Li, X., Liu, L., Schlegel, H.B., 2002. On the physical origin of blue-shifted hydrogen bonds. *J. Am. Chem. Soc.* 124 (32), 9639–9647.
- Lim, T.-G., 2015. 20-O- $\beta$ -D-glucopyranosyl-20 (S)-protopanaxadiol, a metabolite of ginsenoside Rb1, enhances the production of hyaluronic acid through the activation of ERK and Akt mediated by Src tyrosin kinase in human keratinocytes. *Int. J. Mol. Med.* 35 (5), 1388–1394.
- Moon, S.S., 2018. Synthesis of a novel  $\alpha$ -glucosyl ginsenoside F1 by cyclodextrin glucanotransferase and its in vitro cosmetic applications. *Biomolecules* 8 (4), 142.
- Nam, K.Y., Choi, J.E., Park, J.D., 2013. Transformation techniques for the large scale production of ginsenoside Rg3. *Korean J. Med. Crop Sci.* 21 (5), 401–414.
- Noh, K.-H., Oh, D.-K., 2009. Production of the rare ginsenosides compound K, compound Y, and compound Mc by a thermostable  $\beta$ -glycosidase from *Sulfolobus acidocaldarius*. *Biol. Pharm. Bull.* 32 (11), 1830–1835.
- Oh, J.H.L., C, Y., Kim, J.E., Kim, W.H., Seo, J.W., Lim, T.G., et al., 2021. *Effect of characterized green tea extraction Methods and Formulations on enzymatic starch Hydrolysis and intestinal glucose transport*. *Journal of agricultural and food chemistry. J. Agric. Food Chem.* 69 (50), 15208–15217.
- Park, N.-J., et al., 2020. Compound K improves skin barrier function by increasing SPINK5 expression. *J. Ginseng Res.* 44 (6), 799–807.
- Pyo, S.M., Maibach, H.I., 2019. Skin metabolism: relevance of skin enzymes for rational drug design. *Skin Pharmacol. Physiol.* 32 (5), 283–294.
- Quan, L.-H., 2012. Enzymatic transformation of the major ginsenoside Rb2 to minor compound Y and compound K by a ginsenoside-hydrolyzing  $\beta$ -glycosidase from *Microbacterium esteraromaticum*. *J. Ind. Microbiol. Biotechnol.* 39 (10), 1557–1562.
- Ramírez-Hernández, A., Aguilar-Flores, C., Aparicio-Saguilán, A., 2019. Fingerprint analysis of FTIR spectra of polymers containing vinyl acetate. *Dyna* 86 (209), 198–205.
- Shkempi, B., Huppertz, T., 2021. Calcium absorption from food products: food matrix effects. *Nutrients* 14 (1), 180.
- Sun, Z.H., Chen, J., Song, Y.Q., Dou, T.Y., Zou, L.W., Hao, D.C., et al., 2019. Inhibition of human carboxylesterases by ginsenosides: structure–activity relationships and inhibitory mechanism. *Chin. Med.* 14 (1), 1–15.
- Tian, D., et al., 2023. Synthesis of L-aspartic acid-based bimetallic hybrid nanoflowers to immobilize snailase for the production of rare ginsenoside compound K. *J. Mater. Chem. B* 11 (11), 2397–2408.
- Yang, X.D., 2015. A review of biotransformation and pharmacology of ginsenoside compound K. *Fitoterapia* 100, 208–220.
- Yeom, M.H., 2010. The anti-aging effects of Korean ginseng berry in the skin. *Korean J. Pharmacogn.* 41 (1), 26–30.
- Zhou, W., 2008. Development and validation of a reversed-phase HPLC method for the quantitative determination of ginsenosides Rb1, Rd, F2, and compound K during the process of biotransformation of ginsenoside Rb1. *J. Separ. Sci.* 31 (6-7), 921–925, 2008.